

Structural and optical properties of Y and Cu co-doped ZnO sea urchin-like nanostructures

JIA HONG ZHENG^{a,b,*}, SHI FENG NIU^c, WEN XUE ZHANG^a

^a School of Materials Science and Engineering, Chang'an University, Xi'an 710064, Shaanxi Province, P. R. China

^b Key Laboratory of Preparation and Applications of Environmental Friendly Materials of the Ministry of Education, Jilin Normal University, Siping 136000, Jilin Province, P. R. China

^c College Key Laboratory Automotive Transportation Safety Technology Ministry of Communication, Chang'an university, xi'an, 710064, Shaanxi Province, P. R. China

Y and Cu co-doped ZnO sea urchin-like nanostructures were prepared via chemical precipitation method. The co-effects of Y and Cd ions on the optical properties of the as-synthesized samples were studied. Structure and optical properties of sea urchin-like $Zn_{0.93-x}Y_{0.07}Cu_xO$ nanostructures were studied. At Y concentration $x=0.07$ and Cu concentration $x=0.01$, the UV and visible emission intensity reached optimization. Appropriate Y and Cu in ZnO can effectively increase the UV emission and visible emission intensity of ZnO. This enhanced UV and visible emission enables $Zn_{0.93-x}Y_{0.07}Cu_xO$ system potential applications in full light emissions devices.

(Received December 5, 2014; accepted May 7, 2015)

Keywords: Y and Cu co-doped ZnO, Chemical precipitation reduction, Optical properties

1. Introduction

The II-VI semiconductor zinc oxide (ZnO) with a direct wide bandgap (3.37 eV) and a large exciton binding energy (60 meV) has attracted substantial attention in the research community [1-3]. Due to its excellent optical and electrical properties and potential applications, ZnO has been extensively applied in a variety of science and technology fields such as in transistors [2], gas sensors [3], light emitting diodes [4], piezoelectric transducers, phosphors, UV detectors, lasers, and energy-conversion devices [5]. The nanostructures have attracted increasing attention because of their specific properties that differ from their bulk counterparts, and their wide applications in chemistry [8-10], biotechnology [11] and materials science [12]. Currently, there is tremendous enthusiasm in one-dimensional semiconductor nanostructures as building blocks to fabricate nanoscale electronic, optoelectronic, and spintronic devices. ZnO nanowires or nanoneedle are expected to play important roles in these fields.

As one of the most important II-VI semiconductors with wide band gap, ZnO is an environmentally friendly and chemically stable material and is a suitable host material for the doping of transition metal (TM) and rare-earth (RE) ions because of its outstanding photoluminescence properties [13-16].

Previous studies, both experimental and theoretical, showed that ZnO doped with appropriate transition metals (TM) are a most promising candidate for room-temperature ferromagnetism (FM) [17], which have attracted much interest due to their potential applications in spintronics [18]. Moreover, owing to its outstanding optical transparency, doped ZnO has the possibility of studying magneto-optical properties, which could lead to

the development of magneto-optoelectronic devices [19-20]. Recently, as one of diluted magnetic semiconductors (DMSs), Cu doped ZnO materials have attracted intensive interest by the following three facts. First, Cu is a prominent luminescence activator, which can modify the luminescence of ZnO crystals by creating localized impurity levels [21], second, Cu atoms and Cu-related secondary phases are not FM, and therefore, doping Cu may overcome the problem of magnetic precipitates in DMSs. Last, Cu has many physical and chemical properties that are similar to those of Zn, which can change easy the microstructure and the optical properties of the ZnO system [22-23]. Our and other researcher pervious results show that Cu doped ZnO systems have FM properties [24] and also the strong visible-light emissions of ZnO [25].

Meanwhile, ZnO semiconductor nanocrystals are important host materials for doping metallic and rare-earth (RE) ions [26-27]. The RE doped nanocrystals exhibit highly efficient luminescence even at room temperature for their potential use in integrated optoelectronic devices such as visible and infrared luminescent devices [28-29]. It is well known that UV emission in photoluminescence is the main character of ZnO and an intensive UV emission is desirable. However, until now, few experimental studies have focused on the enhance intensity of UV by doping RE or metallic ions into ZnO lattice. Our pervious results show that Y-doped ZnO nanoparticles can effectively increase the UV emission intensity [30]. So, in the present letter, we intend to add two elements of Y and Cu into ZnO crystalline lattice with an expectation that an intensive UV and visible-light emissions would be attained. In this paper, we report a facile and effective chemical precipitation route for fabricating Y and Cu co-

doped ZnO powders and study the structures, photoluminescence (PL) and of the Y and Cu co-doped ZnO powders.

2. Experimental

Zn_{0.93-x}Y_{0.07}Cu_xO powders with $x = 0.00, 0.01, 0.03$ and 0.05 were prepared via the chemical precipitation method. All the chemical reagents used in the experiment were analytical grade purity. Zinc nitrate [Zn(NO₃)₂ · 6H₂O] and appropriate amounts of the stoichiometric quantities of Y(NO₃)₃ · 6H₂O and Cu(NO₃)₂ · 3H₂O were dissolved in deionized water with stirring to form main mixture solution. And the solution of NH₄HCO₃ was added into the main mixture solution gradually. The reaction between the two solutions lasted for 4 hours until adequate white precipitate formed. The white precipitate was filtered and washed with alcohol for several times and then placed a drying oven at 50°C for drying. At last, the dried product was annealed at 400°C for 2 hours to form the final powder.

X-ray diffraction was employed to determine the phase structure, performed on a D/max-Rigaku XRD diffraction spectrometer with a Cu K α line of 1.5417 Å and a monochromator at 50 kV and 300 mA. The room-temperature PL spectra were measured with a fluorescence spectrophotometer using a He-Cd laser with a wavelength of 325 nm as the excitation light source.

3. Results and discussion

The XRD patterns of as-synthesized (Y, Cu) co-doped ZnO samples with different Cu concentrations are presented in Fig. 1. All the peaks in the X-ray diffraction pattern (Fig. 1) are assigned to the typical wurtzite structure of ZnO (JCPDS 36-1451) and those sharp diffraction peaks indicate that the ZnO prepared with the present method are relative highly crystallized.

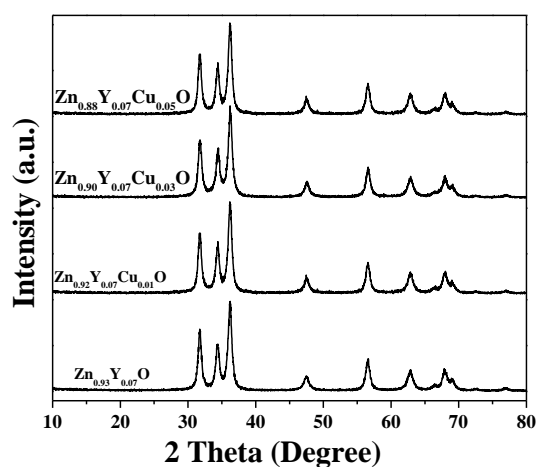


Fig. 1. XRD patterns of Zn_{0.93-x}Y_{0.07}Cu_xO powders with different concentrations ($x = 0.00, 0.01, 0.03, 0.05$).

The typical X-ray diffraction pattern indicates that there are no traces of copper and yttrium oxides, any binary zinc-copper or zinc-yttrium and ternary zinc-copper-yttrium phases have been observed, which indicates no impurity exist in the samples.

The value of lattice volume decreased with increasing Cu doping concentration. The decrease in lattice volume illustrates the substitution of Zn by Cu ions in ZnO lattice, as the ionic radius of Cu (0.57 Å) is smaller than that (0.74 Å) of Zn ion. Due to differences in ionic radius of Zn ions and Cu ions, Cu incorporation will lead to a contraction of the ZnO lattice. These results are in close agreement with the earlier reports [31].

The nearest-neighbor Zn-O bond length along the c -direction is given by [32]

$$L = \sqrt{a^2/3 + (1/2 - u)^2 c^2} \quad (1)$$

where the internal parameter u in wurtzite structure is defined as

$$u = (1/3)(a^2/c^2) + 1/4 \quad (2)$$

It should be noted that there is a strong correlation between the c/a ratio and the u parameter. When the c/a ratio decrease, the u parameter increases in such a way that four tetrahedral distances remain nearly constant through a distortion of tetrahedral angles due to long range polar interactions [33]. Fig. 2 shows plot of calculated Zn-O bond lengths as a function of Zn_{0.93-x}Y_{0.07}Cu_xO nanostructures. It is clear from the Fig. 2 that Zn-O bond lengths decrease linearly with the increase of Cu doping concentration. The changes in the lattice volume and bond length indicated that the Cu ions have been successfully substituted for Zn²⁺ ions in ZnO crystal lattice.

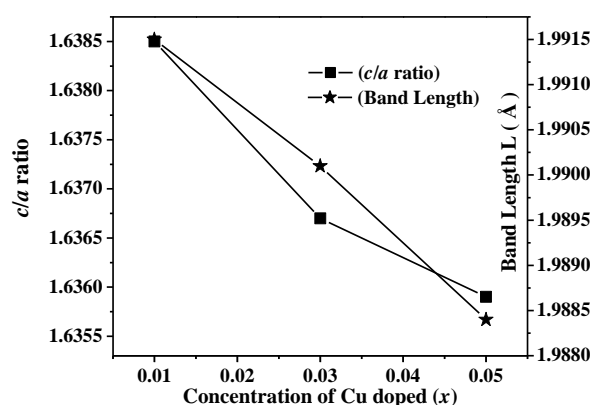


Fig. 2. Shows plot of calculated Zn-O bond lengths and c/a ratio as a function of Zn_{0.93-x}Y_{0.07}Cu_xO nanostructures.

FESEM images of the sea urchin-like Zn_{0.88}Y_{0.07}Cu_{0.05}O nanostructures are presented in Fig. 3. Fig. 3a and b displays the low magnification and high magnification FESEM images of the sea urchin-like Zn_{0.88}Y_{0.07}Cu_{0.05}O nanostructures, respectively. The intact morphology of an individual sea urchin-like ZnO

nanostructure is observed in Fig. 3b. From the FESEM image of ZnO urchin, it is clear that the spheres are assembled by a central nucleus and many needle-like $\text{Zn}_{0.88}\text{Y}_{0.07}\text{Cu}_{0.05}\text{O}$ which grow radially from the nucleus. Length of nanoneedles is at 2-3 μm range and diameter is of 50-100 nm.

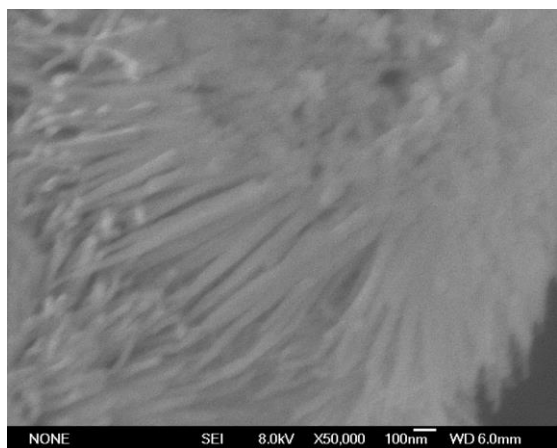
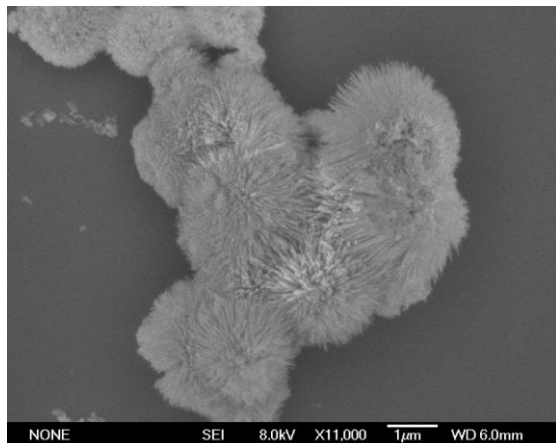


Fig. 3. FESEM images of the sea urchin-like $\text{Zn}_{0.88}\text{Y}_{0.07}\text{Cu}_{0.05}\text{O}$ nanostructures, (a) low magnification, (b) high magnification.

Raman-scattering spectra are sensitive to crystallization, structural disorder, and defects in materials and were therefore used to study the optical properties of $\text{Zn}_{0.88}\text{Y}_{0.07}\text{Cu}_{0.05}\text{O}$ urchin assembled with nanoneedles. According to the group theory, hexagonal wurtzite ZnO belongs to the C_{6v}^4 space group, the optical phonons at the Γ point of the Brillouin zone are $A_1 + 2B_1 + E_1 + 2E_2$ [34-35]. The B_1 modes are silent modes, the A_1 and E_1 modes are polar and exhibit different frequencies for the transverse-optical (TO) and longitudinal-optical (LO) phonon modes. Both A_1 and E_1 are Raman and infrared active, whereas the E_2 modes are nonpolar having two frequencies: E_2 (high) associated with oxygen displacement and E_2 (low) associated with Zn sub-lattice and are Raman active only [36]. Fig. 4 shows the Raman spectra of $\text{Zn}_{0.88}\text{Y}_{0.07}\text{Cu}_{0.05}\text{O}$ urchin synthesized by chemical precipitation method. Peak obtained at 333 cm^{-1} were assigned to the second order Raman scattering due to the zero boundary phonons [37]. The peak at 380 cm^{-1} corresponds to A_1 symmetry with the TO mode and while the peak at 439 cm^{-1} is attributed to ZnO non-polar optical phonons high E_2 mode, confirming the good crystal quality of the as-grown sea urchin-like $\text{Zn}_{0.88}\text{Y}_{0.07}\text{Cu}_{0.05}\text{O}$ nanostructures [38]. Peak at 491 cm^{-1} is

attributed to A_1 (LO) phonons. Peak at 570 cm^{-1} is attributed to E_1 (LO) phonon mode which is indicative of the structural disorder present in the ZnO nanoneedles [39].

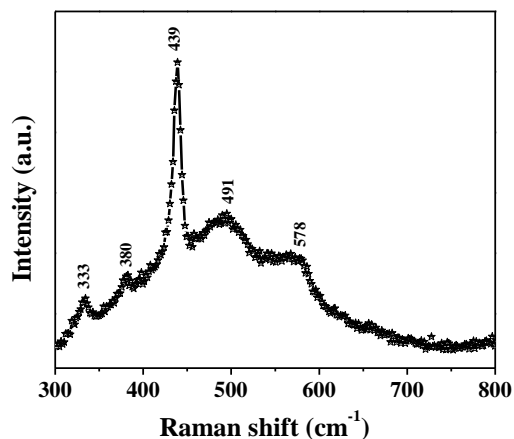


Fig. 4. Shows the typical room temperature Raman spectra of sea urchin-like $\text{Zn}_{0.88}\text{Y}_{0.07}\text{Cu}_{0.05}\text{O}$ nanostructures.

To investigate the effects of Y and Cu co-doping on the optical property samples, the room temperature photoluminescence (PL) spectra are plotted in Fig. 5. The room-temperature PL spectra were measured with a fluorescence spectrophotometer using a He-Cd laser with a wavelength of 325 nm as the excitation light source. Fig. 5(a) shows the photoluminescence (PL) spectra of $\text{Zn}_{1.93-x}\text{Y}_{0.07}\text{Cu}_x\text{O}$ alloys with different Cu doping concentration x . Fig. 5(b) the PL spectrum of $\text{Zn}_{0.93}\text{Y}_{0.07}\text{O}$ is also provided for comparison. It is seen from Fig. 5(a) all the spectra have a distinct peak of ultraviolet (UV) emission originated from the free excitonic recombination, corresponding to near-band-edge (NBE) emission of zinc oxide [40]. When Cu ions as donors are incorporated into $\text{Zn}_{0.93}\text{Y}_{0.07}\text{O}$ systems, the bandgap structure of ZnO nanoparticles will be modulated and new emission centers are formed, which leads to the slight lower wavelength shift in the UV emission. The peak positions of PL spectra are significantly dependent on the size of the ZnO crystalline due to the quantum-confinement effect, which will induce the gap enhancement [41]. The size of ZnO nanoparticles decrease in our case. So the blue-shift for the UV emission may be related to the quantum-confinement effect of the ZnO nanoparticles [41]. Meanwhile, the intensity of UV emission decreased with the increase of Cu doping concentration. The results agree with the previous research results [25].

It can also be seen that all of the doped ZnO samples exhibit a strong and broad deep level emission (DLE) peak in the visible region. The intensity of visible emission increased first and then decreased. Cu doping into ZnO lattice can effectively enhance the visible emission ($x=0.01, 0.03$). When Cu concentration increases to $x=0.03$, the peak intensity UV and visible emission decreases. Therefore, in this PL spectrum, the optical property of $\text{Zn}_{0.92}\text{Y}_{0.07}\text{Cu}_{0.01}\text{O}$ is best. First, doping of Y into ZnO lattice will reduce the quantity of nonradiative recombination centers, and hence decrease the

nonradiative recombination and enhance radiative recombination, strengthening the UV emission. And then, this Cu impurity center behaves like a trap for nonequilibrium holes or electrons. As a carrier is trapped, the Cu impurity center acquires a charge with respect to the lattice, and a long-range Coulomb field arises in addition to the short-range potential of the isoelectronic impurity. This field promotes electron or hole trapping onto a weakly localized hydrogen-like orbital. Ultimately probability of failure in the recombination of holes and electrons is enhanced i.e., non radiative excitonic transitions from defect states become more prevalent [42]. Therefore, Cu doping into ZnO lattice can effectively enhance the visible emission. Our pervious results show that Y-doped ZnO nanoparticles can effectively increase the UV emission intensity [30] and Cu doped ZnO systems can strong the visible-light emissions of ZnO [25]. In this paper, Y and Cu co-doped ZnO can keep excellent optical property of the single element (Y or Cu) doping, which enhance the intensity of UV or visible emission of ZnO. This easy and effective method for enhancing the UV and visible emission, may lead to the development of ZnO for application in full light emissions.

4. Conclusions

In conclusion, we have investigated the structure and optical properties in sea urchin-like nanostructures of $\text{Zn}_{1.93-x}\text{Y}_{0.07}\text{Cu}_x\text{O}$ by chemical precipitation method. XRD and Raman results demonstrated that Y and Cu ions were successfully incorporated into the lattice of ZnO. With increasing Cu doping concentration, ZnO lattice volume decreased. Photoluminescence spectrum reveals that doping of Y and Cu in ZnO can effectively increased the UV emission and visible emission intensity of ZnO. Both UV and visible emission intensity increased of ZnO may lead to the development of ZnO for application in full light emissions.

Acknowledgements

The project was supported by the Special Fund for Basic Scientific Research of Central Colleges, Chang'an University (NO. 0009-2014G1311083 and NO. 0009-2014G1221017) and the Applications of Environmental Friendly Materials from the Key Laboratory Ministry of Education, Jilin Normal University.

References

- [1] A. B. Djuricic, X. Y. Chen, Y. H. Leung, A. M. C. Ng, *J. Mater. Chem.* **22**, 6526 (2012).
- [2] M. M. Brewster, X. Zhou, M. Y. Lu, S. Gradecak, *Nanoscale* **4**, 1455 (2012).
- [3] S. F. Nelson, D. H. Levy, L. W. Tutt, *Appl. Phys. Lett.* **101**, 183503 (2012).
- [4] M. S. Arnold, P. Avouris, Z. W. Pan, Z. L. Wang, *J. Phys. Chem. B* **107**, 659 (2003).
- [5] H. T. Wang, B. S. Kang, F. Ren, L. C. Tien, P. W. Sadik, D. P. Norton, S. J. Pearton, J. Lin, *Appl. Phys. Lett.* **86**, 243503 (2005).
- [6] P. J. Pauzauskie, P. Yang, *Mater. Today* **9**, 36 (2006).
- [7] Y. Qin, X. D. Wang, Z. L. Wang, *Nature* **451**, 809 (2008).
- [8] P. M. Ajayan, O. Stephan, C. Colliex, et al., *Science* **265**, 1212 (1994).
- [9] S. Banerjee, S. S. Wong, *Nano Lett.* **2**, 195 (2002).
- [10] H. J. Shin, D. K. Jeong, J. G. Lee, et al., *Adv. Mater.* **16**, 1197 (2004).
- [11] V. Ghormade, M. V. Deshpande, K. M. Paknikar, *Biotechnol. Adv.* **29**, 792 (2011).
- [12] D. K. Samarakoon, X. Q. Wang, *ACS Nano* **4**, 4126 (2010).
- [13] D. Katsuki, T. Sato, R. Suzuki, Y. Nanai, S. Kimur, T. Okuno, *Appl. Phys. A* **108**, 321 (2012).
- [14] W. C. Hao, J. J. Li, H. Z. Xu, J. O. Wang, T. M. Wang, *Prog. Nat. Sci.* **21**, 31 (2011).
- [15] G. X. Gu, G. Xiang, J. Luo, H. T. Ren, M. Lan, D. W. He, X. Zhang, *J. Appl. Phys.* **112**, 023913 (2012).
- [16] J. Lang, X. Li, J. Yang, L. Yang, Y. Zhang, Y. Yan, Q. Han, M. Wei, M. Gao, X. Liu, R. Wang, *Appl. Surf. Sci.* **257**, 9574 (2011).

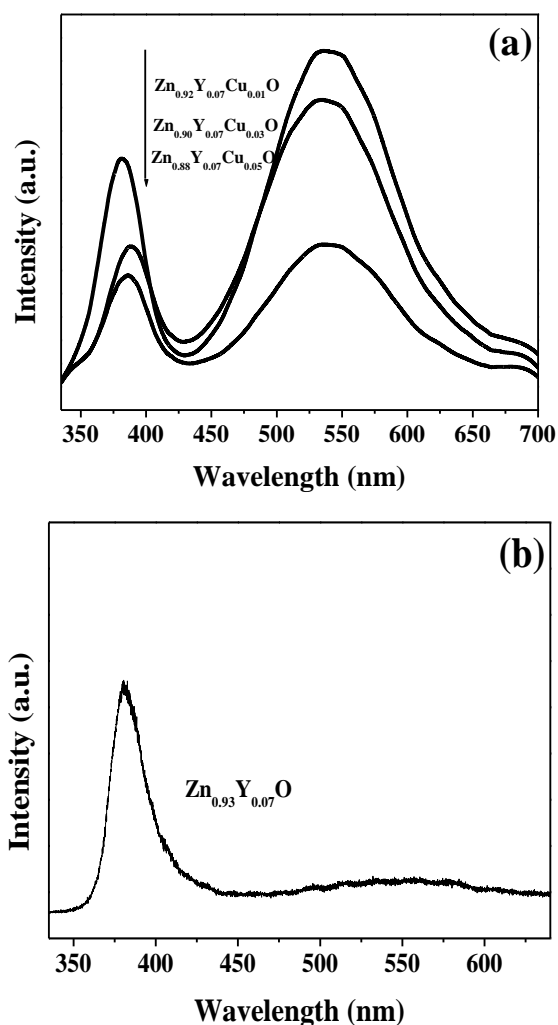


Fig. 5. PL spectra of $\text{Zn}_{0.93-x}\text{Y}_{0.07}\text{Cu}_x\text{O}$ sea urchin-like nanostructures with different Cu doping concentrations.

- [17] R. Janisch, P. Gopal, N.A. Spaldin, *J. Phys.: Condens. Matter* **17**, R657 (2007).
- [18] S. A. Wolf, D. D. Awschalom, R. A. Buhrman, J. M. Daughton, S. V. Molnar, M. L. Roukes, A. Y. Chtchelkanova, D. M. Treger, *Science* **294**, 1488 (2001).
- [19] A. I. Savchuk, A. Perrone, A. Lorusso, et al., *Appl. Surf. Sci.* **302**, 205 (2014).
- [20] R. E. Nowak, M. Vehse, O. Sergeev, T. Voss, M. Seyfried, et al., *Advanced Optical Materials*, **2**, 94 (2014).
- [21] H. L. Liu, X. Cheng, H. B. Liu, J. H. Yang, et al., *Superlattices and Microstructures* **52**, 1171 (2012).
- [22] Y. Darma, Tun Seng Herng, R. Marlina, et al., *Appl. Phys. Lett.* **104**, 081922 (2014).
- [23] T. M. Hammad, J. K. Salem, R. G. Harrison, et al., *J. Mater. Sci.: Mater. El.* **24**, 2846 (2013).
- [24] J. H. Zheng, J. L. Song, X. J. Li, Q. Jiang, J. S. Lian, *Crystal Research and Technology* **46**, 1143 (2011).
- [25] J. H. Zheng, J. L. Song, Q. Jiang, J. S. Lian, *J. Mater. Sci.: Mater. El.* **23**, 1521 (2012).
- [26] B. K. Grandhel, V. R. Bandi, K. W. Jang, et al., *Journal of Nanoscience and Nanotechnology* **13**, 7680 (2013).
- [27] Y. Yang, Y. P. Li, C. X. Wang, et al. *Advanced Optical Materials* **2**, 240 (2014).
- [28] L. Armelao, F. Heigl, A. Jurgensen, R. I. R. Blyth, T. Regier, X. T. Zhou, T. K. Sham, *J. Phys. Chem. C* **111**, 10194 (2007).
- [29] R. Zamiri, A. Kaushal, A. Rebelo, et al. *Ceramics International* **40**, 1635 (2014).
- [30] J. H. Zheng, J. L. Song, Q. Jiang, J. S. Lian, *Appl. Surf. Sci.* **258**, 6735 (2012).
- [31] J. Anghel, A. Thurber, D. A. Tenne, C. B. Hanna, A. Punnoose, *J. Appl. Phys.* **107**, 09E314 (2010).
- [32] C. S. Barret, T. B. Massalski, *Structure of Metals* (Pergamon Press, Oxford, 1980).
- [33] H. Morkoc, U. Ozgur, *Zinc Oxide: Fundamentals, Materials and Device Technology* (Willey- VCH Verlag GmbH & Co. KGaA, Weinheim, 2009).
- [34] L. W. Yang, X. L. Wu, G. S. Huang, T. Qiu, Y. M. Yang, *J. Appl. Phys.* **97**, 014308 (2005).
- [35] H. C. Zhu, J. Iqbal, H. J. Xu, J. Yu, *Chem. Phys.* **129**, 124713 (2008).
- [36] Z. W. Peng, G. Z. Dai, W. C. Zhou, P. Chen, Q. Wan, et al., *Appl. Surf. Sci.* **256**, 6814 (2010).
- [37] A. Umar, Y. B. Hahn, *Nanotechnology* **17**, 2174 (2006).
- [38] B. Kumar, H. Gong, S. Y. Chow, S. Tripathy, *Appl. Phys. Lett.* **89**, 71922 (2006).
- [39] L. Liao, D. H. Liu, J. C. Li, C. Liu, Q. Fu, M. S. Ye, *Appl. Surf. Sci.* **240**, 175 (2005).
- [40] Y. C. Kong, D. P. Yu, B. Zhang, et al., *Appl. Phys. Lett.* **78**, 407 (2001).
- [41] H. L. Liu, J. H. Yang, Z. Hua, et. al, *J. Mater. Sci.: Mater. Electron.* **23**, 832 (2012).
- [42] Kousik Samanta, A. K. Arora, Ram S. Katiyar, *J. Appl. Phys.* **110**, 043523 (2011).

*Corresponding author: jhzheng@chd.edu.cn